

Fast-response IR spatial light modulators with a polymer network liquid crystal

Fenglin Peng^a, Haiwei Chen^a, Suvagata Tripathi^b, Robert J. Twieg^b, and Shin-Tson Wu^{*a}

^aCollege of Optics and Photonics, University of Central Florida, Orlando, Florida, USA 32816

^bDepartment of Chemistry, Kent State University, Kent, Ohio, USA 44242

ABSTRACT

Liquid crystals (LC) have widespread applications for amplitude modulation (e.g. flat panel displays) and phase modulation (e.g. beam steering). For phase modulation, a 2π phase modulo is required. To extend the electro-optic application into infrared region (MWIR and LWIR), several key technical challenges have to be overcome: 1. low absorption loss, 2. high birefringence, 3. low operation voltage, and 4. fast response time. After three decades of extensive development, an increasing number of IR devices adopting LC technology have been demonstrated, such as liquid crystal waveguide, laser beam steering at $1.55\mu\text{m}$ and $10.6\mu\text{m}$, spatial light modulator in the MWIR ($3\sim 5\mu\text{m}$) band, dynamic scene projectors for infrared seekers in the LWIR ($8\sim 12\mu\text{m}$) band. However, several fundamental molecular vibration bands and overtones exist in the MWIR and LWIR regions, which contribute to high absorption coefficient and hinder its widespread application. Therefore, the inherent absorption loss becomes a major concern for IR devices. To suppress IR absorption, several approaches have been investigated: 1) Employing thin cell gap by choosing a high birefringence liquid crystal mixture; 2) Shifting the absorption bands outside the spectral region of interest by deuteration, fluorination and chlorination; 3) Reducing the overlap vibration bands by using shorter alkyl chain compounds. In this paper, we report some chlorinated LC compounds and mixtures with a low absorption loss in the near infrared and MWIR regions. To achieve fast response time, we have demonstrated a polymer network liquid crystal with 2π phase change at MWIR and response time less than 5 ms.

Keywords: Fast response time, Infrared (IR), spatial light modulators, polymer network liquid crystal, low absorption, high birefringence.

1. INTRODUCTION

Liquid crystals (LCs) are widely used in the visible [1, 2], infrared (IR) [3, 4], millimeter wave [5], and terahertz [6, 7] spectral regions. Both amplitude modulation (such as displays [8]) and phase modulation (e.g., tunable prism for laser beam steering [9] and adaptive lenses [10]) have been investigated extensively. For intensity modulation, twisted nematic [11], in-plane switching [12], and vertical alignment [13] have been used in display devices. But for phase modulation, 2π phase modulo is generally required so that homogeneous alignment with a positive Δn LC is preferred [14]. The phase change (δ) of a homogeneous cell is governed by the cell gap (d) and wavelength (λ) as:

$$\delta = 2\pi d \Delta n / \lambda. \quad (1)$$

In the visible region, say $\lambda=0.5\mu\text{m}$, this condition can be easily satisfied but in the mid-wave infrared (MWIR, $\lambda=3\sim 5\mu\text{m}$) region, say $\lambda=5\mu\text{m}$, the required $d\Delta n$ is $\sim 10\text{X}$ larger than that at $\lambda=0.5\mu\text{m}$. Moreover, as the wavelength increases, Δn decreases and then gradually saturates [15]. Thus, a fairly large cell gap is needed, which leads to slow response time. To achieve sub-millisecond response time, a polymer network liquid crystal (PNLC) has been explored at $\lambda=1.06\mu\text{m}$ and $1.55\mu\text{m}$ [16, 17]. In a PNLC, the phase change is determined by $d\Delta n$ (Eq. (1)), but the response time is governed by the average domain size [18]. Thus, the phase change is decoupled from the response time. Though the small domain size increases operating voltage, it helps to suppress light scattering and shorten response time effectively.[19].

In order to increase Δn without sacrificing good UV stability, we can extend the conjugation length by adding phenyl rings to the core. However, the use of too many phenyl rings would result in some undesirable properties: 1) the melting point is too high and its solubility in a LC host is very limited [7]; 2) its viscosity increases dramatically, and 3) its birefringence gradually saturates once there are more than three phenyl rings. Therefore, terphenyls (three rings) could be an optimal conjugation length [20].

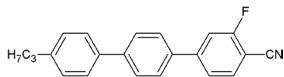
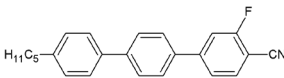
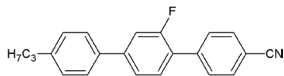
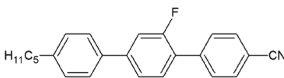
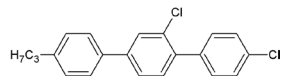
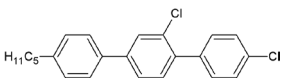
For IR applications, another important factor needs to be considered, which is absorption originating from vibration of molecular bonds and functional groups. From absorption viewpoint, the $\pi \rightarrow \pi^*$ electronic transitions of a conjugated LC occur in the UV region. [21] As the molecular conjugation increases, the resonance wavelength increases gradually. In the visible to near infrared ($\sim 1 \mu\text{m}$) region, most LCs are quite transparent. As the wavelength keeps increasing, molecular vibrations, e.g., CH stretching, CN stretching, C=C stretching in the phenyl rings, C-H in-plane deformation, C-C skeletal stretching, C-F stretching, and C-H out-of-plane deformation, etc. take place in the mid-wave infrared (MWIR 3-5 μm) and long-wave infrared (LWIR 8-12 μm) regions. In MWIR, several notable molecular vibration bands exist, such as CH, CH₂, CH₃, CN, C=C, and NCS stretching. The CH, CH₂, and CH₃ absorption bands overlap closely and form a strong absorption band covering from 3.2 μm to 3.7 μm . [22] These carbon-hydride bonds in the alkyl chain or in the aromatic rings are basic elements for an organic compound to exhibit mesogenic phase. On the other hand, the narrow but strong cyano (CN) and tolane (C=C) absorption peaks occur at $\sim 4.45 \mu\text{m}$ while isothiocyanato (NCS) polar group has a broad and strong absorption band in the 4.5-5.2 μm region. Therefore, to reduce absorption loss, several approaches have been investigated: 1) Shifting the absorption bands outside the spectral region of interest by deuteration [23, 24], fluorination [25], or chlorination [26]. 2) Reducing the cell gap by using a high Δn LC mixture. 3) Choosing a proper polar group. Although NCS provides a large Δn and $\Delta \epsilon$ while keeping a modest viscosity, its characteristic vibration absorption band is strong and broad in the 4.5-5.2 μm spectral range [22]. Thus, NCS compounds are not desirable for MWIR applications. On the other hand, CN has a strong dipole moment and it is compatible to monomers for making PNLC devices. Although its absorption peak at $\sim 4.45 \mu\text{m}$ is strong, its bandwidth is relatively narrow. Therefore, high transmittance in the off-resonance region can still be achieved. Fluoro and chloro polar groups offer high resistivity, good UV stability, and modest dipole moment [27-29] and they are widely used in thin-film transistor LC displays [30].

In this paper, we report a terphenyl LC mixture, which shows high birefringence ($\Delta n=0.34$ at $\lambda=514\text{nm}$ and $\Delta n=0.253$ at $\lambda=4\mu\text{m}$), high transmittance ($T>98\%$) in the MWIR region, and broad nematic range. Using this mixture, we fabricated three PNLC devices. The PNLC result holds promise for MWIR applications, especially its response time is about 100X faster than that of the nematic LC host.

2. LC COMPOUNDS AND MIXTURES FOR MWIR

We prepared two series of terphenyl compounds as listed in Table 1. Compounds 1 through 4 are fluorinated cyano-terphenyls. The phase transition temperatures were measured by Differential Scanning Calorimetry (DSC). As shown in Table 1, these cyano compounds exhibit a fairly high melting point. Compounds 5 and 6 are chlorinated terphenyls, which show a fairly low absorption and modest birefringence at MWIR. In order to further lower the melting point while maintaining high Δn , we made the LC mixture, which is designated the final mixture as M1. To our surprise, the melting point of M1 drops to below -40°C (limited by our DSC) and its clearing point is 149.7°C . Thus, M1 shows an extraordinarily broad nematic range.

Table 1. Chemical structures and phase transition temperatures of the seven terphenyl compounds employed. T_{mp} represents melting point and T_c clearing point.

Compound #	Chemical structure	T_{mp} (°C)	T_c (°C)
1		109	199
2		86	183
3		91	208
4		93	191
5		95	68
6		71	65

3. PHYSICAL PROPERTIES

We prepared a homogeneous cell with a cell gap $d \approx 5 \mu\text{m}$ to characterize the physical properties of M1. The ITO (indium tin oxide) glass substrates were over-coated with a thin polyimide (PI) layer rubbed in anti-parallel directions to create a 3° pretilt angle and strong anchoring energy. The cell was filled with M1 and mounted in a Linkam LTS 350 Large Area Heating/Freezing Stage controlled by TMS94 Temperature Programmer. Birefringence was determined by measuring the voltage-dependent transmittance (VT) of the homogeneous cell sandwiched between two crossed linear polarizers. To achieve maximum transmittance, the LC director was oriented at 45° with respect to the transmission axis of polarizer. A tunable Argon-ion laser ($\lambda=457, 488, \text{ and } 514\text{nm}$), He-Ne laser ($\lambda=633\text{nm}$) and a semiconductor laser ($\lambda=1550\text{nm}$) were used as light sources. A 1 kHz square-wave AC signal was applied to the LC cell and the transmitted light was measured by a photodiode and recorded by a LabVIEW data acquisition system (DAQ, PCI16110).

3.1 Birefringence

The birefringence can be obtained at a given temperature from Eq. (1) using the VT curve and the wavelength and cell gap. We measured the temperature dependence of the Δn of M1 from 25°C to 130°C and the results for $\lambda=633\text{nm}$ are plotted in Fig. 1. Circles in Fig. 1 are experimental data and solid line is a fit with Haller's semi-empirical equation [31]:

$$\Delta n = \Delta n_0 (1 - T/T_c)^\beta, \quad (2)$$

where Δn_0 stands for the extrapolated birefringence at $T=0\text{K}$ and β is a material constant. Through fitting, we found $\Delta n_0 = 0.38$ and $\beta = 0.19$.

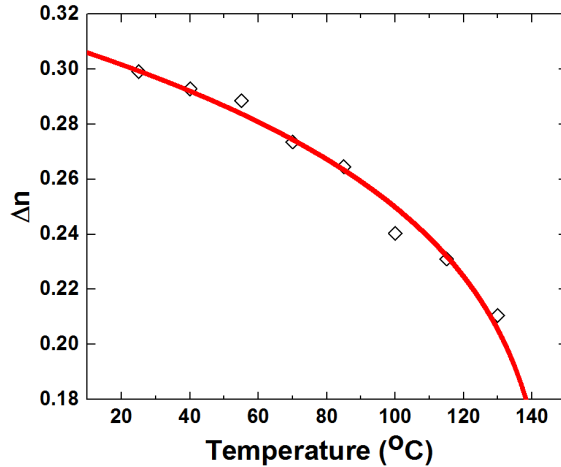


Fig. 1. Temperature dependent birefringence of M1 at $\lambda=633\text{nm}$: the circles are measured data and the red line is a fitting curve with Eq. (2).

Fig. 2 shows the birefringence dispersion of M1. The red line is the fitting curve given by the single-band birefringence dispersion equation where G is a proportionality constant and λ^* is the mean resonance wavelength. [15]

$$\Delta n = G \frac{\lambda^2 \lambda^{*2}}{\lambda^2 - \lambda^{*2}}, \quad (3)$$

Through fitting, we found $G=3.78 \mu\text{m}^{-2}$ and $\lambda^*=0.258 \mu\text{m}$. Based on these parameters, the birefringence at any wavelength can be calculated. According to Fig. 2, the birefringence decreases to a plateau and its value is about 10%~20% lower in the MWIR region. For M1, its birefringence remains relatively high ($\Delta n=0.253$) at $\lambda=4\mu\text{m}$. Based on $\Delta n=0.253$, we found that the required cell gap for $\delta=2\pi$ at $\lambda=4\mu\text{m}$ is about $16\mu\text{m}$. High Δn enables a thin cell gap to be used for achieving 2π phase change, which in turn improves transmittance and response time in the MWIR region.

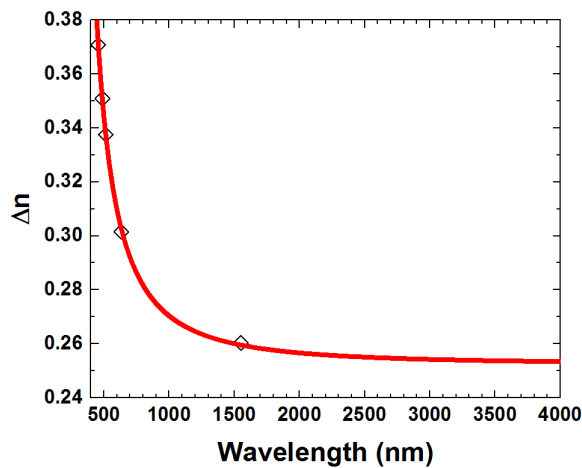


Fig. 2. Birefringence dispersion of M1 at room temperature: circles are measured data and solid line is fitting with Eq. (3).

3.2 MWIR transmittance

We fabricated a LC cell using two barium fluoride (BaF_2) substrates as well to measure the transmittance at MWIR. The BaF_2 is transparent from UV to $10\mu\text{m}$ and its refractive index decreases with wavelength from 1.5 to 1.4 [32]. At $\lambda=4\mu\text{m}$, the refractive index of BaF_2 is about 1.457. We did not measure the individual refractive indices (n_e and n_o) of M1 in the MWIR region, but based on the E7 data ($n_o \approx 1.50$) [33] we estimated that $n_e \approx 1.77$ and $n_o \approx 1.51$ for M1. To align M1, we spin-coated a thin PI layer on the inner surface of the BaF_2 substrate and gently rubbed the PI layers. Thus, the LC

molecules are homogeneously aligned to eliminate light scattering at room temperature. Due to a limited choice of spacers in our lab, we fabricated a LC cell with $d=24\mu\text{m}$ instead of the targeted $16\mu\text{m}$. The transmittance spectrum was measured by FTIR (Perkin Elmer Spectrum One FTIR Spectrometer) at RT. Fig. 3 shows the measured transmission spectrum. Although there is a strong absorption peak at $\lambda=4.45\mu\text{m}$ due to the CN vibration as expected [3, 34], its bandwidth is relatively narrow. The baseline transmittance in the off-resonance region is higher than 98%.

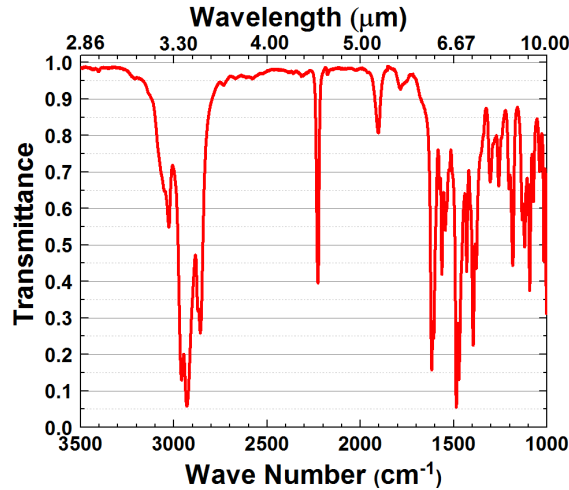


Fig. 3. Measured transmittance spectrum of M1 in the MWIR region with cell gap $d=24\mu\text{m}$.

3.3 Dielectric anisotropy

We measured the capacitance of a homogeneous cell and a homeotropic cell using an HP-4274 multi-frequency LCR meter to determine dielectric anisotropy. For M1, we found $\Delta\epsilon=19.6$ at room temperature and 1 kHz. The cyano and chlorine polar groups contribute to this modest dielectric anisotropy.

3.4 Visco-elastic constant

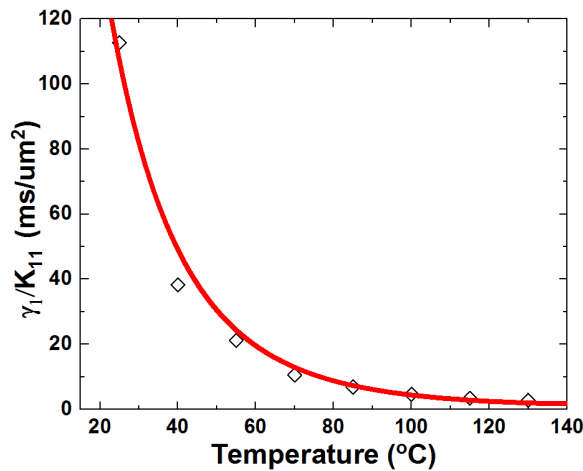


Fig. 4. Temperature dependent visco-elastic coefficients of M1: circles are measured data and red line is fitting with Eq. (6). $\lambda=633\text{nm}$.

The visco-elastic coefficient (γ_1/K_{11}) was obtained by measuring the transient free relaxation time for a controlled phase change where δ_0 stands for the total phase change, which needs to be kept small in order to satisfy the small angle approximation:

$$\delta(t) = \delta_0 \exp(-2t/\tau_0), \quad (4)$$

$$\tau_0 = \gamma_1 d^2 / (K_{11} \pi^2), \quad (5)$$

In Eq. (5), τ_0 is the LC director relaxation time, γ_1 is the rotational viscosity, and K_{11} is the splay elastic constant. Figure 4 depicts the temperature dependent visco-elastic coefficient of M1. At room temperature (22°C), $\gamma_1/K_{11}=113 \text{ ms}/\mu\text{m}^2$. The relatively large visco-elastic constant results from the rigid terphenyl cores, the cyano group and some heavy chlorine substitutions. As the temperature increases, the visco-elastic coefficient decreases dramatically. The solid line in Fig. 4 is theoretical fitting with following equation [35]:

$$\frac{\gamma_1}{K_{11}} = A \frac{\exp(E_a / k_B T)}{(1 - T/T_c)^\beta}, \quad (6)$$

Here A is a proportionality constant, E_a is the activation energy, T is the Kelvin temperature, and k_B is the Boltzmann constant. For M1, we found $A=4.33 \times 10^{-6} \text{ ms}/\mu\text{m}^2$ and $E_a=432.04 \text{ meV}$. As expected, such a large viscosity would lead to a slow response time. For instance, if M1 is employed in a reflective-mode LC cell with $d=12 \mu\text{m}$, the estimated optical decay time is 830 ms, which is too slow for laser beam steering applications. However, high viscosity is particularly desirable for making polymer network liquid crystal (PNLC) devices with small domain sizes because of its slow diffusion rate, as will be described in detail next.

4. POLYMER NETWORK LIQUID CRYSTAL

In order to fabricate PNLCs, we prepared precursors by mixing M1 with monomer RM257 (Merck) and photo-initiator BAPO (Genocure). Here, we used the mesogenic monomer RM257 to maintain good alignment and obtain spatially uniform phase profile [18]. Next, we filled the precursor into a homogeneous LC cell (ITO glass). The cell gap was $11.8 \mu\text{m}$ and the cell was operated in reflective mode in order to obtain 2π phase change at $\lambda=4 \mu\text{m}$ and lower operation voltage. A thin cell gap helps to reduce operation voltage [16] because

$$V_{2\pi} \sim \frac{d}{d_1} \sqrt{\frac{K_{11}}{\epsilon_0 \Delta \epsilon}}, \quad (7)$$

where d_1 is the average domain size, ϵ_0 is electric permittivity, and $\Delta \epsilon$ is dielectric anisotropy. In the UV curing process, we controlled the sample temperature at 0°C to obtain small domain size [19]. Small domain size helps to suppress light scattering (this is particularly important in the visible spectral region) and achieve fast response time, but a trade-off is increased $V_{2\pi}$ as described in Eq. (7). A UV light-emitting diode (LED) lamp ($\lambda=385 \text{ nm}$, intensity=300 mW/cm²) was used to cure the precursors and the exposure time was one hour. M1 is a good PNLC host because both the terphenyl core and terminal groups (-CN and -Cl) are UV stable and provide a relatively large viscosity.

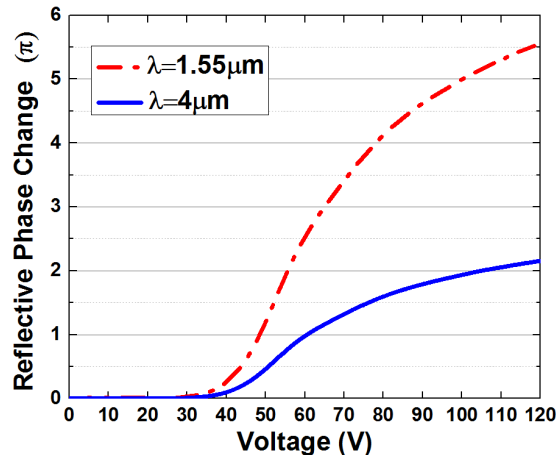


Fig. 5. The voltage-dependence phase change curves of PNLC sample in a reflective mode at $\lambda=1.55 \mu\text{m}$ and $\lambda=4 \mu\text{m}$, respectively. Cell gap $d=11.8 \mu\text{m}$.

We measured the VT curve at $\lambda=1.55\mu\text{m}$ to characterize the electro-optical properties of our PNLC cells, because our ITO glass substrates are not transparent and its transmittance drops to 60% at $\lambda=4\mu\text{m}$ [36]. The PNLC cell was sandwiched between two crossed polarizers, with the rubbing direction at 45° to the polarizer's transmission axis. We converted the measured VT curve to a voltage-dependent phase (VP) curve for each sample. Figure 5 shows the VP curve for the PNLC with 5 wt% of RM257. According to the dispersion curve shown in Fig. 2, the birefringence is insensitive to the wavelength in the IR region. Therefore, based on Eq. (1) we converted the VP curve from $\lambda=1.55\mu\text{m}$ to $\lambda=4\mu\text{m}$. To measure the response time of a PNLC, we removed the biased voltage spontaneously at $t=0$. The biased voltage was 105V, corresponding to $V_{2\pi}$ at $\lambda=4\mu\text{m}$. The measured phase decay time (from 100% to 10%) fits Eq. (4) well (data not shown here). The decay time is only 3.6ms, which is $\sim 230X$ faster than that of the LC host. This fast response time is critically important for the MWIR laser beam steering devices. For MWIR applications, highly transparent substrates and electrodes are required. The thickness of alignment layer is less than 80nm and thus its absorption is negligible. Regarding to substrates, BaF_2 is quite transparent ($>95\%$) from UV to $10\mu\text{m}$. For transparent electrodes, we could consider a thin carbon nanotube layer [37], graphene, or meshed metal wires [38].

5. CONCLUSION

A terphenyl LC mixture has been developed, which shows high birefringence ($\Delta n=0.34$ at 514nm and $\Delta n=0.253$ at $4\mu\text{m}$), good UV stability, and a very broad nematic range (from -40°C to 146.3°C). High birefringence enables a thin cell gap to be used for achieving a 2π phase change at MWIR, while keeping high transmittance ($T>98\%$) and low operation voltage. To achieve fast response time, we also have demonstrated a polymer network liquid crystal with 2π phase change at MWIR and response time is only 3.6ms.

ACKNOWLEDGMENT

The authors are indebted to Office of Naval Research for the financial support under contract No. N00014-13-1-0096.

REFERENCES

- [1] Yang, D.-K. and Wu, S.-T., *Fundamentals of Liquid Crystal Devices* (John Wiley & Sons, 2006).
- [2] Lueder, E., *Liquid Crystal Displays: Addressing Schemes and Electro-optical Effects* (John Wiley & Sons, 2010).
- [3] Wu, S.-T., "Infrared properties of nematic liquid crystals: an overview," *Opt. Eng.* **26**(2), 120-128 (1987).
- [4] Peng, F., Chen, H., Tripathi, S., Twieg, R. J., and Wu, S.-T., "Fast-response infrared phase modulator based on polymer network liquid crystal," *Opt. Mater. Express*, 265-273 (2015).
- [5] Lim, K. C., Margerum, J. D., and Lackner, A. M., "Liquid crystal millimeter wave electronic phase shifter," *Appl. Phys. Lett.* **62**(10), 1065-1067 (1993).
- [6] Lin, X., Wu, J., Hu, W., Zheng, Z., Wu, Z., Zhu, G., Xu, F., Jin, B., and Lu, Y., "Self-polarizing terahertz liquid crystal phase shifter," *AIP Adv.* **1**(3), 032133 (2011).
- [7] Dąbrowski, R., Kula, P., and Herman, J., "High birefringence liquid crystals," *Crystals* **3**(3), 443-482 (2013).
- [8] Peng, F., Chen, Y., Yuan, J., Chen, H., Wu, S.-T., and Haseba, Y., "Low temperature and high frequency effects on polymer-stabilized blue phase liquid crystals with large dielectric anisotropy," *J. Mater. Chem. C* **2**(18), 3597-3601 (2014).
- [9] Efron, U., *Spatial Light Modulator Technology: Materials, Devices, and Applications* (Marcel Dekker, 1994), Vol. 47.
- [10] Ren, H. and Wu, S.-T., *Introduction to Adaptive Lenses* (Wiley, 2012).
- [11] Schadt, M. and Helfrich, W., "Voltage-dependent optical activity of a twisted nematic liquid crystal," *Appl. Phys. Lett.* **18**(4), 127-128 (1971).
- [12] Soref, R. A., "Transverse field effects in nematic liquid crystals," *Appl. Phys. Lett.* **22**(4), 165-166 (1973).
- [13] Schiekkel, M. F. and Fahrenschon, K., "Deformation of nematic liquid crystals with vertical orientation in electrical fields," *Appl. Phys. Lett.* **19**(10), 391-393 (1971).
- [14] Wu, S.-T., Efron, U., and Hsu, T.-Y., "Near-infrared-to-visible image conversion using a Si liquid-crystal light valve," *Opt. Lett.* **13**(1), 13-15 (1988).
- [15] Wu, S.-T., "Birefringence dispersions of liquid crystals," *Phys. Rev. A* **33**(2), 1270 (1986).

- [16] Sun, J., Xianyu, H., Chen, Y., and Wu, S.-T., "Submillisecond-response polymer network liquid crystal phase modulators at 1.06- μm wavelength," *Appl. Phys. Lett.* **99**(2), 021106 (2011).
- [17] Fan, Y.-H., Lin, Y.-H., Ren, H., Gauza, S., and Wu, S.-T., "Fast-response and scattering-free polymer network liquid crystals for infrared light modulators," *Appl. Phys. Lett.* **84**(8), 1233-1235 (2004).
- [18] Sun, J. and Wu, S. T., "Recent advances in polymer network liquid crystal spatial light modulators," *J. Polym. Sci., Part B: Polym. Phys.* **52**(3), 183-192 (2014).
- [19] Sun, J., Wu, S.-T., and Haseba, Y., "A low voltage submillisecond-response polymer network liquid crystal spatial light modulator," *Appl. Phys. Lett.* **104**(2), 023305 (2014).
- [20] Schadt, M., "Liquid crystal materials and liquid crystal displays," *Annu. Rev. Mater. Sci.* **27**(1), 305-379 (1997).
- [21] Wu, S.-T., "Absorption measurements of liquid crystals in the ultraviolet, visible, and infrared," *Journal of applied physics* **84**(8), 4462-4465 (1998).
- [22] Mistry, B., *A Handbook of Spectroscopic Data Chemistry: UV, IR, PMR, CNMR and Mass Spectroscopy* (Oxford Book Company, 2009).
- [23] Gray, G. W. and Mosley, A., "The synthesis of deuteriated 4-n-alkyl-4'-cyanobiphenyls," *Mol. Cryst. Liq. Cryst.* **48**(3-4), 233-242 (1978).
- [24] Wu, S.-T., Wang, Q.-H., Kempe, M. D., and Kornfield, J. A., "Perdeuterated cyanobiphenyl liquid crystals for infrared applications," *J. Appl. Phys.* **92**(12), 7146-7148 (2002).
- [25] Chen, Y., Xianyu, H., Sun, J., Kula, P., Dabrowski, R., Tripathi, S., Twieg, R. J., and Wu, S.-T., "Low absorption liquid crystals for mid-wave infrared applications," *Opt. Express* **19**(11), 10843-10848 (2011).
- [26] Peng, F., Chen, Y., Wu, S.-T., Tripathi, S., and Twieg, R. J., "Low loss liquid crystals for infrared applications," *Liq. Cryst.* **41**(11), 1545-1552 (2014).
- [27] Wu, S.-T., Coates, D., and Bartmann, E., "Physical properties of chlorinated liquid crystals," *Liq. Cryst.* **10**(5), 635-646 (1991).
- [28] Schadt, M., "Field-effect liquid-crystal displays and liquid-crystal materials: key technologies of the 1990s," *Displays* **13**(1), 11-34 (1992).
- [29] Hird, M., "Fluorinated liquid crystals—properties and applications," *Chem. Soc. Rev.* **36**(12), 2070-2095 (2007).
- [30] Chen, Y., Luo, Z., Peng, F., and Wu, S.-T., "Fringe-field switching with a negative dielectric anisotropy liquid crystal," *J. Disp. Technol.* **9**(2), 74-77 (2013).
- [31] Haller, I., "Thermodynamic and static properties of liquid crystals," *Prog. Solid State Chem.* **10**(103-118) (1975).
- [32] Malitson, I. H., "Refractive properties of barium fluoride," *JOSA* **54**(5), 628-630 (1964).
- [33] Li, J., Wu, S.-T., Brugioni, S., Meucci, R., and Faetti, S., "Infrared refractive indices of liquid crystals," *J. Appl. Phys.* **97**(7), 073501 (2005).
- [34] Wu, S.-T., "Infrared markers for determining the order parameters of uniaxial liquid crystals," *Appl. Opt.* **26**(16), 3434-3440 (1987).
- [35] Knepe, H., Schneider, F., and Sharma, N. K., "Rotational viscosity γ_1 of nematic liquid crystals," *J. Chem. Phys.* **77**(6), 3203-3208 (1982).
- [36] Khoo, I.-C. and Wu, S.-T., *Optics and Nonlinear Optics of Liquid Crystals* (World Scientific, 1993).
- [37] Zhang, M., Fang, S., Zakhidov, A. A., Lee, S. B., Aliev, A. E., Williams, C. D., Atkinson, K. R., and Baughman, R. H., "Strong, transparent, multifunctional, carbon nanotube sheets," *Science* **309**(5738), 1215-1219 (2005).
- [38] Hecht, D. S., Hu, L., and Irvin, G., "Emerging transparent electrodes based on thin films of carbon nanotubes, graphene, and metallic nanostructures," *Adv. Mater.* **23**(13), 1482-1513 (2011).